ACS Medicinal Chemistry Letters

ACS AuthorChoice

LETTER

pubs.acs.org/acsmedchemlett

Metabolism of 4-Aminopiperidine Drugs by Cytochrome P450s: Molecular and Quantum Mechanical Insights into Drug Design

Hao Sun* and Dennis O. Scott

Department of Pharmacokinetics, Dynamics and Metabolism, Pfizer Inc., Groton, Connecticut 06340, United States

Supporting Information

ABSTRACT: 4-Aminopiperidines are a variety of therapeutic agents that are extensively metabolized by cytochrome P450s with CYP3A4 as a major isoform catalyzing their N-dealkylation reaction. However, its catalytic mechanism has not been fully elucidated in a molecular interaction level. Here, we applied theoretical approaches including the molecular mechanics-based docking to study the binding patterns and quantum mechanics-based reactivity calculations. They were supported by the experimental human liver microsomal clearance and P450 isoform phenotyping data. Our results herein suggested that the molecular interactions between substrates and CYP3A4 active site residues are essential for the N-dealkylation of 4-aminopiperidines. We also found that the serine 119 residue of CYP3A4 may serve as a key hydrogen-bonding partner to interact with the 4-amino groups of the studied drugs. The reactivity of the side chain α-carbon hydrogens drives the direction of catalysis as well. As a result, structure-based drug design approaches look promising to guide drug discovery programs into the optimized drug metabolism space.

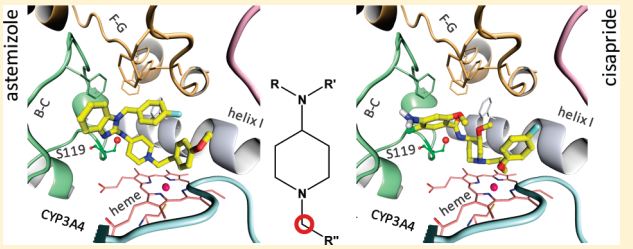

KEYWORDS: Cytochrome P450, drug metabolism, N-dealkylation, 4-aminopiperidine, CYP3A4, drug design

Alicyclic amines are common chemical moieties of small-molecule therapeutic agents. Their metabolic fates include ring α-oxidation to lactams, N-oxidation, the N-dealkylation of the side chain α-carbon, and ring-opening reactions,[1] which have been extensively investigated. In principle, these reactions are catalyzed by cytochrome P450s but sometimes also by other phase I drug-metabolizing enzymes such as flavin-containing monooxygenase. Previous in vitro and clinical studies on the metabolism of the drugs containing a 4-aminopiperidine moiety, the typical alicyclic amine serving as a synthetic linker (sometimes also pharmacologically active), pointed out that it is the N-dealkylation reaction that occurred predominantly rather than other piperidine ring-related biotransformation pathways as described above.[2] At the moment, the therapeutic agents sharing a 4-aminopiperidine moiety include astemizole, bamipine, benperidol, bezitramide, cisapride, clebopride, domperidone, enzastaurin, fentanyl, indoramin, lorcainide, α-methylfentanyl, pimozide, sabeluzole, and timiperone (Figure 1), which act on diverse drug targets (Table 1). Our primary objective was to elucidate the molecular mechanisms of their metabolic fate by P450s with a focus on N-dealkylation reactions.

N-Dealkylation is a typical biotransformation pathway in P450-catalyzed oxygenation reactions, which are initiated from the binding of substrates into the enzyme active site pocket. It is followed by exposing the reaction center of substrates to the heme iron for the catalytic electron transfer from cofactors such as NADPH (nicotinamide adenine dinucleotide phosphate, reduced form) and reductase. Interestingly, most of these piperidine moieties are located in the middle region of the studied molecular structures, which suggests that their conformation has to be altered to expose the side-chain α-carbon hydrogen(s) to the heme for the abstraction by P450 compound I catalytic species, a rate-limiting step for N-dealkylation reactions.[3] Theoretically, other molecular mechanisms may also exist such as a direct nitrogen atom oxidation. However, no previous studies have focused on the molecular mechanisms of the N-dealkylation reaction of these 4-aminopiperidine drugs. There are good reasons to hope that the mechanistic information extracted from this study may guide us into rational drug design and redesign from the perspective of drug metabolism.

Here, we applied theoretical approaches including the quantum mechanics-based density functional theory (DFT) to calculate the activation energy of the α-carbon radical intermediate formation and the molecular mechanics-based docking method to simulate the substrate binding modes to P450s. In particular, a series of 4-aminopiperidine fragments in simulating their corresponding drugs were designed to calculate the side-chain α-carbon hydrogen atom abstraction to address the impact of the electronic properties of various substitution groups. Likewise, the effects of the molecular interactions between substrates and P450 active site residues on their metabolic fate were investigated by the docking of 4-aminopiperidine drugs directly into CYP3A4, the major isoform for their N-dealkylation reactions. Some key metabolic end points were lacking or not well characterized in previous studies, so experimental methods including the half-life-based human liver microsomal clearance determination and the phenotyping identification of P450 isoforms were incorporated

Received: May 11, 2011
Accepted: June 18, 2011
Published: June 18, 2011

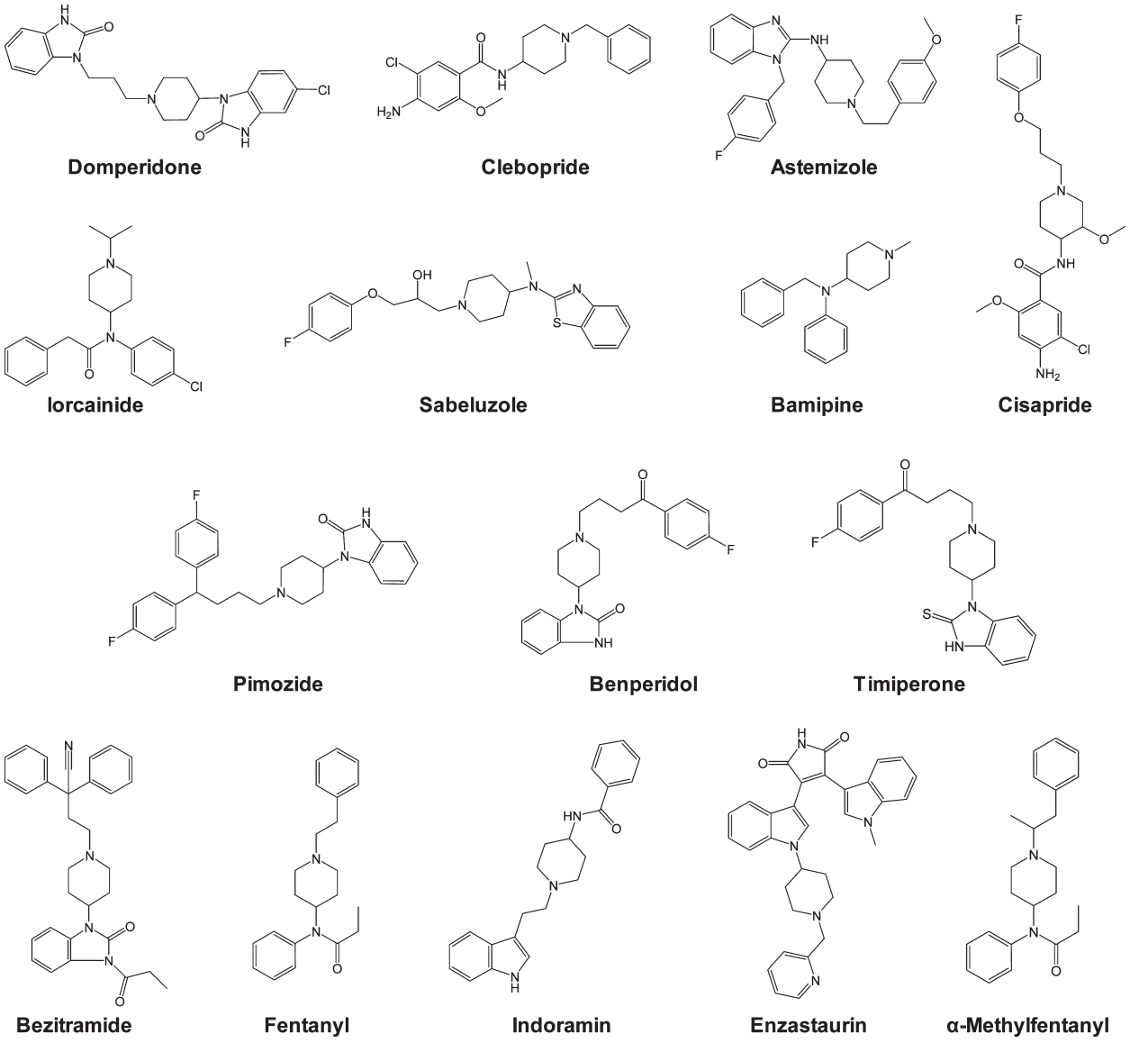

Figure 1. Chemical structures of 4-aminopiperidine therapeutic agents.

in this study as well. The combined approaches led us to elucidate the overall and individual mechanisms of the metabolic fate of the studied 4-aminopiperidine drugs, especially their N-dealkylation reactions.

Overall, the human liver microsomal clearance results indicated that these 4-aminopiperidine drugs have moderate to high clearance, indeed, high clearance for a majority of them. CYP3A4 was found to be a major isoform for the metabolism of these drugs with the exception of indoramin, lorcainide, and sabeluzole. For them, CYP2D6 also contributed significantly. These findings are supported by our in vitro phenotyping experiments (Table 1) that measured the disappearance rate constant of the tested compounds with recombinant enzymes CYP1A2, 2B6, 2C8, 2C9, 2C19, 2D6, and 3A4 and further confirmed by the CYP inhibitor studies. However, CYP3A4 was indeed the major isoform for the N-dealkylation of all studied 4-aminopiperidines (CYP2D6 catalyzes totally different reactions such as an aromatic hydroxylation as discussed below). Hence, we chose CYP3A4 to model the substrate binding to elucidate the mechanism of the N-dealkylation of 4-aminopiperidines. It demonstrated that the N-dealkylation orientation is one of the lowest energy binding clusters but not necessarily the lowest one. This is quite understandable given the fact that some lowest energy binding clusters may account for other pharmacological and biological processes besides metabolism and catalysis, for example, the enzyme inhibition. It appears that several structural regions of CYP3A4 have close interactions with 4-aminopiperidines, including its B−C loop (R105, R106, P107, F108, S119, and I120), F−G loop (R212, F213, F215, and F241), I helix (I301, F304, A305, and T309), K−β region (I369, A370, M371, R372, L373, and E374), and several residues at its β3 sheets (G481, L482, and L483). In particular, the substituents at the 4-amino end of 4-aminopiperidines tend to bind toward the B−C and F−G loops, and those at the piperidine ring nitrogen side bind toward the K−β region along the I helix of CYP3A4. More importantly, the predicted N-dealkylation binding poses also suggested a crucial role of the 4-amino nitrogen atom, which was found to sit closely (3−4 Å) to the oxygen atom of the serine 119's hydroxyl group at the

dx.doi.org/10.1021/ml200117z |ACS Med. Chem. Lett. 2011, 2, 638–643

Table 1. Therapeutic and Metabolic Profiles of 4-Aminopiperidine Drugs

4-aminopiperidine therapeutics	main indication[2]	mechanism[2]	N-dealkylation[2,4,5,8−18]	active metabolite by N-dealkylation[2]	P450 for N-dealkylation	half-life ($t_{1/2}$) of parent compound depletion from phenotyping assay	microsomal clearance (μL/min/mg)
astemizole	antihistaminic	nonsedating type histamine H_1-receptor antagonist	minor	active	CYP3A4	3A4 (1.5 m), 2D6 (4.0 m), others (>60 m)	136.0 ± 13.5 (n = 8)
bamipine	antihistaminic	sedating type histamine receptor antagonist	major	undetermined	unknown	N/A	N/A
benperidol	antipsychotic	butyrophenone cerebral dopamine receptor blocker	major	undetermined	CYP3A4	3A4 (3.3 m), 2D6 (10.4 m), 2C8 (43.8 m), others (>60 m)	42.0 ± 1.7 (n = 4)
bezitramide	analgesic	opioid	major	undetermined	unknown	N/A	N/A
cisapride	gastroprokinetic	serotonin 5-HT_4 receptor agonist	major	1/6 active	CYP3A4	3A4 (<5 m), others (>60 m)	120.7 ± 5.8 (n = 13)
clebopride	antiemetic; antispasmodic	dopamine receptor antagonist	major	active	CYP3A4	3A4 (<5 m), others (>60 m)	50.4 ± 3.3 (n = 9)
domperidone	antiemetic; gastroprokinetic	dopamine D_2-receptor antagonist	major	not active	CYP3A4	3A4 (<5 m), 2D6 (58 m), others (>60 m)	108.6 ± 6.1 (n = 13)
enzastaurin	antineoplastic	protein kinase C-β inhibitor	major	active	CYP3A	N/A	N/A
fentanyl	analgesic	prototype anilidopiperidine opioid	major	not active	CYP3A4	N/A	32.3 ± 3.1 (n = 3)
indoramin	antihypertensive	α_1 adrenoceptor antagonist	minor	undetermined	CYP3A4	2D6 (<5 m), 3A4 (16.0 m), others (>60 m)	46.4 ± 7.6 (n = 9)
lorcainide	antiarrhythmic	type IC	minor	active	CYP3A4	2D6 (4.7 m), 3A4 (27.9 m), 2C19 (57.0 m), others (>60 m)	159.0 ± 58.8 (n = 12)
α-methyl-fentanyl	analgesic	designer drug of fentanyl, opioid	major	not active	unknown	N/A	N/A
pimozide	antipsychotic	diphenylbutylpiperidine class	major	undetermined	CYP3A4	3A4 (2.7 m), 2D6 (3.2 m), others (>60 m)	57.0 ± 24.0 (n = 12)
sabeluzole	nootropic	N-methyl D-aspartate receptor antagonist	minor	undetermined	CYP3A4	2D6 (1.5 m), 3A4 (<5.0 m), others (>60 m)	37.0 ± 1.2 (n = 3)
timiperone	antipsychotic	butyrophenone cerebral dopamine receptor blocker	major	not active	unknown	N/A	N/A

B−C loop of CYP3A4 in an energetically favored orientation to form a strong hydrogen bond. With this key force, 4-aminopiperidines are juxtaposed above the heme porphyrin ring to expose their α-carbon hydrogens to P450 compound I (3−4 Å between the α-carbon and the heme iron of CYP3A4). For a comprehensive analysis of these findings in the hope of elucidating their catalytic mechanisms individually, 4-aminopiperidines were categorized into several structural subgroups according to the type and size of these substituents connected to the piperidine ring nitrogen atom.

4-Aminopiperidines in the first group are those equipped with small-sized aliphatic substituents such as the methyl, ethyl, and isopropyl moieties. Metabolic studies of the antihistamine drug bamipine found that its major metabolites are *N*-desmethylbamipine and a *para*-hydroxylated product at the *N*-benzyl ring.[4] In another study, the biotransformation of lorcainide came up with a major metabolic pathway via its terminal phenyl ring hydroxylation by CYP2D6 ($t_{1/2}$ = 4.7 min). However, the N-dealkylation was still catalyzed by CYP3A4 ($t_{1/2}$ = 27.9 min), but its metabolite norlorcainide might be a relatively minor product (Table 1).[5] Jointly, lorcainide is extensively metabolized by human liver microsomes (159 μL/min/mg). Considering the small molecular size of bamipine and lorcainide and relatively big active site cavity of CYP3A4 has led us to reason that their catalytic rates are driven more likely by the reactivity of the α-carbon hydrogens. As we observed from the docking studies, the N-phenyl rings of bamipine and lorcainide bind toward the phenylalanine clusters located at the B−C and F−G loops of CYP3A4, but the relatively large gap between them prevents $\pi-\pi$ interactions. They also lack the molecular interactions with the K−β loop of CYP3A4 (Figure 2). On the other hand, the DFT calculations demonstrated that the α-carbon hydrogen activation energy of the methyl, ethyl, and isopropyl 4-aminopiperidines are 98.47, 96.64, and 96.55 kcal/mol (Table 2), respectively, a reasonable range for P450-catalyzed oxygenation reactions.[6,7]

Clebopride and enzastaurin are a group of 4-aminopiperidines with a methylene linker connecting the piperidine ring nitrogen atom and a bulky aromatic moiety, that is, phenyl and pyridine, respectively. Our docking results indicated that these aromatic rings appear to slide along the I helix toward the K−β loop and hence to drag the α-carbons above the heme iron (Figure 2). The activation energy of clebopride's α-carbon hydrogen is dramatically decreased (−13.17 kcal/mol) as compared to its methylated analogue, which suggests that its radical form is stabilized by the resonance effect, that is, the electron donating from the *p* system of the adjacent aromatic ring. Clebopride is mainly metabolized via an N-dealkylation pathway to *N*-desbenzylclebopride[8] and extensively metabolized by CYP3A4 and human liver microsomes (50 μL/min/mg). Likewise, the replacement of the benzene moiety with a pyridine ring (like enzastaurin) further lowers the activation potential (−4.70 kcal/mol to N-benzyl and −17.87 kcal/mol to N-methyl analogues) (Table 2). It is expected that the developing anticancer drug enzastaurin is predominantly metabolized via an N-demethylenepyridine pathway.[9]

Astemizole, fentanyl/α-methylfentanyl, and indoramin are another group of 4-aminopiperidine drugs. They differentiate from the rest because of their ethylene linker. Likewise, to expose their α-carbon hydrogens for N-dealkylation, the derivatives at the other end of the ethylene linker are subject to certain torsional angle restrictions that arise from the hindrance of the

dx.doi.org/10.1021/ml200117z |*ACS Med. Chem. Lett.* 2011, 2, 638–643

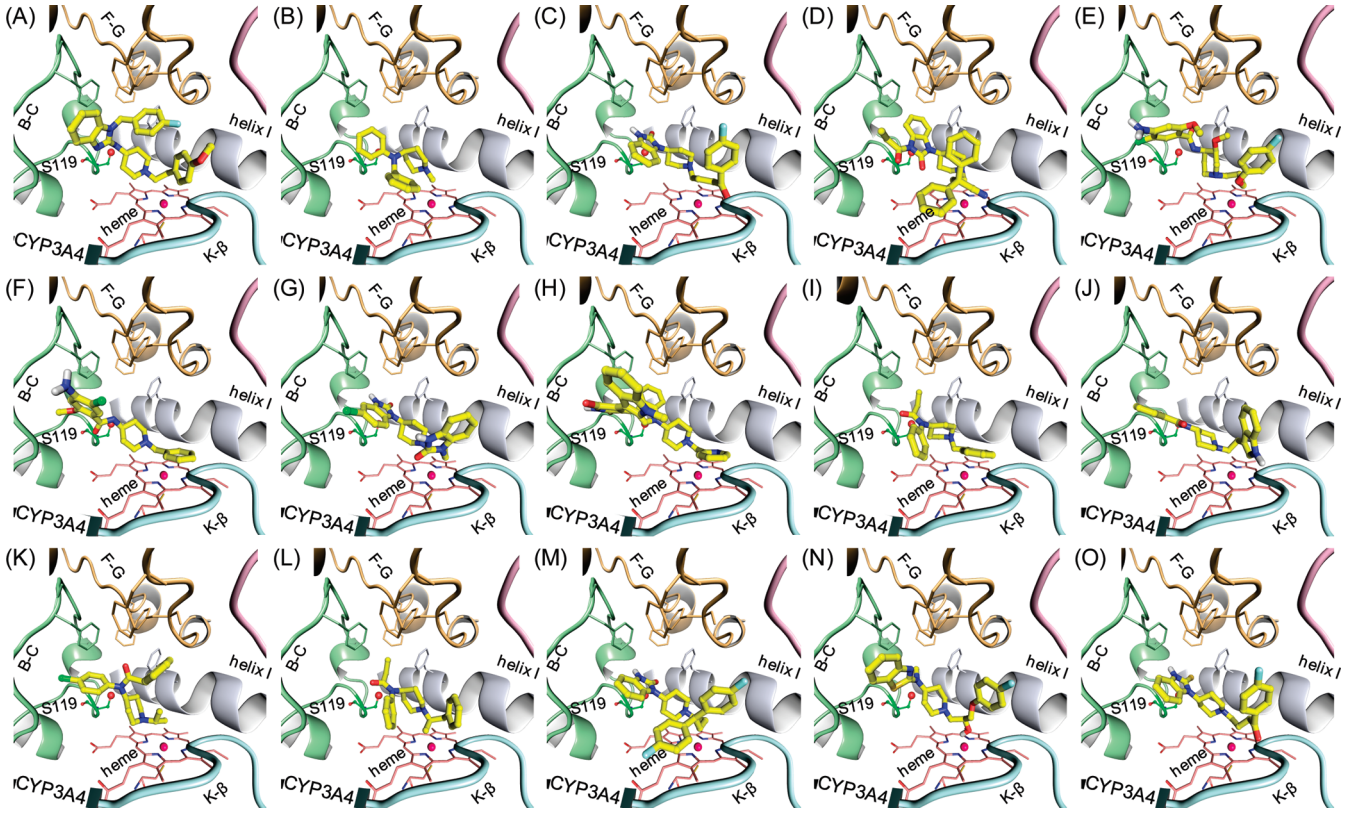

Figure 2. Proposed N-dealkylation binding poses of 4-aminopiperines, (A) astemizole, (B) bamipine, (C) benperidol, (D) bezitramide, (E) cisapride, (F) clebopride, (G) domperidone, (H) enzastaurin, (I) fentanyl, (J) indoramin, (K) lorcainide, (L) α-methylfentanyl, (M) pimozide, (N) sabeluzole, and (O) timiperone. Conformation and orientation are generated by AutoDock and selected from one of the lowest energy binding poses and illustrated using PyMOL. Essential active site regions are colored and marked.

Table 2. Quantum Chemical Calculation of the α-Carbon Hydrogen Atom Abstraction of 4-Aminopipyridine Fragments Using the DFT/B3LYP 6-31G Method**

4-Aminopiperidine Fragments	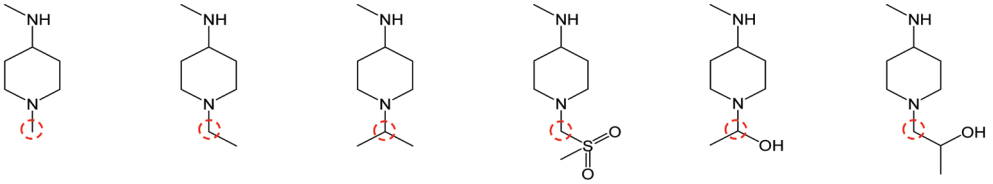					
Original Energy (hartree)	-385.867030	-425.181005	-464.493416	-973.751945	-500.387852	-539.699969
Radical Energy (hartree)	-385.209830	-424.526727	-463.839288	-973.100505	-499.737991	-539.046403
Activation Energy (kcal/mol)	**98.47**	**96.64**	**96.55**	**94.86**	**93.87**	**96.19**
4-Aminopiperidine Fragments	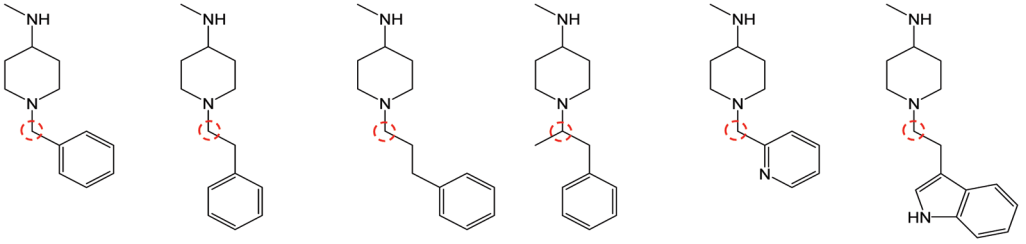					
Original Energy (hartree)	-616.911006	-656.229485	-695.536906	-695.538877	-632.950474	-787.796725
Radical Energy (hartree)	-616.274801	-655.575174	-694.886168	-694.889052	-632.321752	-787.143015
Activation Energy (kcal/mol)	**85.30**	**96.66**	**94.42**	**93.85**	**80.60**	**96.28**

neighboring I helix and heme porphyrin. It is highly unlikely that the *trans* conformation of these substrates exists, which otherwise would push the aromatic end groups penetrating into the heme porphyrin ring. It turned out that the measured

dx.doi.org/10.1021/ml200117z |*ACS Med. Chem. Lett.* 2011, 2, 638–643

dihedral angles tend to adopt a *gauche*-like conformation (but not exactly 60 degrees), that is, an eclipsed conformation close to 90 degrees (Figure 2). The activation energy of their α-carbon hydrogen(s) is very close to those of direct aliphatic chain substitution and hence much less affected by the aromatic ring's resonance effects (Table 2). Previous studies pointed out that CYP3A4-catalyzed N-dealkylation of indoramin, which has an indole moiety connected to the ethylene linker, is a relatively minor metabolic pathway, as compared to CYP2D6-catalyzed indole 6-hydroxylation reaction.[10] This may be explained by the unfavored torsional rotation by the bulky indole substitution. Indeed, this phenomenon also applies to the second-generation antihistamine astemizole, a drug for the treatment of allergic rhinitis. Its major metabolite is *O*-desmethylastemizole (67% conversion from astemizole) that is catalyzed by CYP2D6 and 2J2. However, its N-dealkylated metabolite norastemizole (or tecastemizole) and the benzimidazole hydroxylated metabolite are only 9 and 25% converted from astemizole, respectively, which are catalyzed by CYP3A4 predominantly.[11] On the other hand, for smaller end group substitution at the ethylene linker, such as fentanyl, the typical binding mode described above is energetically favored consistently; hence, its N-dealkylated metabolite norfentanyl was found to be a major metabolite by CYP3A4 (~50% turned over from the parent compound),[12] but its human liver microsomal clearance is moderate to high (32 μL/min/mg, Table 1). To further explore the effect of other steric variation of the ethylene linker, for example, to add a methyl group to its α-carbon, we found that its activation energy is lowered (−2.81 kcal/mol, Table 2), but this effect may be concealed since the methyl group per se hinders the exposure of the α-carbon hydrogen presumably. Take α-methylfentanyl, a designer drug of fentanyl by the methylation of its α-carbon. It was demonstrated that its N-dealkylated metabolite (nor-fentanyl) is a major metabolite like fentanyl but has a lower turnover rate (24%).[13]

With three or more "linear" aliphatic carbons connected to the piperidine ring nitrogen atom, it appears that the steric hindrance of the bulky substituents of 4-aminopiperidine drugs may be avoided because of these flexible linkers. Their N-dealkylation orientations fit well into those CYP3A4 functional regions such as the B−C loop, F−G loop, I helix, and K−β loop in an energetically favored manner (Figure 2). Take timiperone and benperidol, both of which are the butyrophenone class antipsychotic drugs for the treatment of schizophrenia. They tend to be exclusively metabolized via N-dealkylation.[14,15] Likewise, the N-dealkylation is a major pathway for pimozide metabolism.[16] Similarly, domperidone is mainly metabolized by the N-dealkylation, with its hydroxylated metabolites at the benzimidazolone ring also observed.[17] In addition, cisapride is mainly metabolized by the CYP3A4 via N-dealkylation to norcisapride, which is interestingly a stereoselective reaction that prefers the (+)-cisapride more than the (−)-cisapride enantiomer.[18] Moreover, the analgesic bezitramide and the nootropic sabeluzole are also CYP3A4 substrates for N-dealkylation reactions.

In summary, our study suggested that N-dealkylation is indeed one major route for the 4-aminopiperidine metabolism by P450s and CYP3A4 is a major contributor. Importantly, we found that their 4-amino group serves as a hydrogen bond donor or acceptor to interact with the hydroxyl group of the serine 119 residue at the B−C loop region of CYP3A4 to juxtapose the piperidine moiety in proximity to the heme porphyrin for catalysis theoretically. Indeed, serine 119 is a key active site residue to potentially stabilize the transition state carbon radicals of substrates as supported by previous site-directed mutagenesis studies.[19,20] In addition, the reactivity of the side chain α-carbon hydrogen(s) next to the piperidine ring nitrogen, that is, the stability of their radical species formed, drives the directions of catalysis as well. As a result, the electronic properties of the substituents linked to the α-carbon may be important determining factors; for example, both aliphatic donating and aromatic resonance effects of substitution may facilitate P450-catalyzed catalysis. The reactivity of other aliphatic carbons at the piperidine rings, namely, 2-, 3-, and 4-position carbons, was also calculated by the same DFT methods, but these values seemed not to be impacted significantly by the substitutions listed in Table 2. For example, these values for the N-methyl and N-benzyl analogues are 96.68, 106.29, 94.79, and 94.29, 104.71, 94.57 kcal/mol, respectively, in that order. Also, it appears that the direct access of the piperidine rings to the heme of CYP3A4 is not energetically favored because of steric hindrance. All of this has meant that molecular interactions between 4-aminopiperines and CYP3A4 active site residues especially those direct interactions from the B−C loop, F−G loop, K−β region, and I helix are essential to orient substrates at an appropriate position for catalysis. Yet, despite that serine 119 was not a flexible active site residue as observed during the X-ray cocrystallization with structurally different substrates bound,[6] it is indeed a key residue to control the catalysis of 4-aminopiperidines.

Furthermore, 4-aminopiperine drugs are high-clearance compounds because of their reactive side chain α-carbon atoms. For example, the human liver microsomal clearances of astemizole and cisapride are 136 and 121 μL/min/mg, respectively. It is noticeable that astemizole was recalled in 1999 because of drug−drug interactions, a direct result of its high hepatic clearance by P450s. Other withdrawn drugs for a similar reason were terfenadine (in 1998), mibefradil (in 1998), and cisapride (in 2000). Interestingly, the N-dealkylated active metabolite of astemizole, tecastemizole, was further developed, but unfortunately, the program was terminated after the new drug application with a "not approvable" decision from FDA for additional concerns of pharmacokinetics and safety issues. In addition, two indoramin analogues were designed and synthesized in this study by blocking either the piperidine side chain α-carbon or its 5-position aromatic carbon at the indole ring, with a hydroxyl group. We found that their human liver microsomal clearance was dropped from 46, down to 11 and 16 μL/min/mg, respectively. As expected, physicochemical properties (such as lipophilicity), electronic properties, and substrate binding orientations are all important factors to determine the microsomal clearance. Therefore, combining these factors into drug design schemes should help us achieve better pharmacokinetic and metabolic profiles to expand the chemical space of lead compounds. Hopefully, structure-based drug design approaches are reliable tools to fulfill these goals in the near future.

■ ASSOCIATED CONTENT

Supporting Information. Experimental procedures and supporting results. This material is available free of charge via the Internet at http://pubs.acs.org.

■ AUTHOR INFORMATION

Corresponding Author

*Tel: 860-686-0099. Fax: 860-686-8581. E-mail: hao.sun@pfizer.com.

■ ACKNOWLEDGMENT

We thank Pfizer high-throughput ADME screening groups at both Groton and Sandwich for experimental support in human liver microsomal clearance and CYP phenotyping assays.

■ REFERENCES

(1) Gorrod, J. W.; Aislaitner, G. The metabolism of alicyclic amines to reactive iminium ion intermediates. *Eur. J. Drug Metab. Pharmacokinet.* **1994**, *19* (3), 209–217.

(2) Drug Approvals and Databases, U.S. Food and Drug Administration, http://www.fda.gov/Drugs/InformationOnDrugs.

(3) Ortiz de Montellano, P. R.; De Voss, J. J. Substrate Oxidation by Cytochrome P450 Enzymes. In *Cytochrome P450: Structure, Mechanism, and Biochemistry*, 3rd ed.; Ortiz de Montellano, P. R., Ed.; Kluwer Academic/Plenum Publishers: New York, 2005.

(4) Neidlein, R.; Kleiser, M. Biotransformation and pharmacokinetics of bamipine in rats. 1. biotransformation. *Arzneimittelforschung* **1987**, *37* (1), 32–37.

(5) Meuldermans, W.; Hurkmans, R.; Swysen, E.; Hendrickx, J.; Thijssen, J.; Lauwers, W.; Heykants, J. Excretion and metabolism of lorcainide in rats, dogs and man. *Eur. J. Drug Metab. Pharmacokinet.* **1983**, *8* (4), 335–349.

(6) Sun, H.; Scott, D. O. Structure-based drug metabolism predictions for drug design. *Chem. Biol. Drug Des.* **2010**, *75* (1), 3–17.

(7) Sun, H.; Sharma, R.; Bauman, J.; Walker, D. P.; Aspnes, G. E.; Zawistoski, M. P.; Kalgutkar, A. S. Differences in CYP3A4 catalyzed bioactivation of 5-aminooxindole and 5-aminobenzsultam scaffolds in proline-rich tyrosine kinase 2 (PYK2) inhibitors: retrospective analysis by CYP3A4 molecular docking, quantum chemical calculations and glutathione adduct detection using linear ion trap/orbitrap mass spectrometry. *Bioorg. Med. Chem. Lett.* **2009**, *19* (12), 3177–3182.

(8) Huizing, G.; Beckett, A. H.; Segura, J.; Bakke, O. M. Metabolism of clebopride in vitro. Mass spectrometry and identification of products of amide hydrolysis and N-debenzylation. *Xenobiotica* **1980**, *10* (3), 211–218.

(9) Mukohara, T.; Nagai, S.; Koshiji, M.; Yoshizawa, K.; Minami, H. Phase I dose escalation and pharmacokinetic study of oral enzastaurin (LY317615) in advanced solid tumors. *Cancer Sci.* **2010**, *101* (10), 2193–2199.

(10) Pierce, D. M. A review of the clinical pharmacokinetics and metabolism of the alpha 1-adrenoceptor antagonist indoramin. *Xenobiotica* **1990**, *20* (12), 1357–1367.

(11) Matsumoto, S.; Yamazoe, Y. Involvement of multiple human cytochromes P450 in the liver microsomal metabolism of astemizole and a comparison with terfenadine. *Br. J. Clin. Pharmacol.* **2001**, *51* (2), 133–142.

(12) Feierman, D. E.; Lasker, J. M. Metabolism of fentanyl, a synthetic opioid analgesic, by human liver microsomes. Role of CYP3A4. *Drug Metab. Dispos.* **1996**, *24* (9), 932–939.

(13) Sato, S.; Suzuki, S.; Lee, X. P.; Sato, K. Studies on 1-(2-phenethyl)-4-(N-propionylanilino)piperidine (fentanyl) and related compounds VII. Quantification of alpha-methylfentanyl metabolites excreted in rat urine. *Forensic Sci. Int.* **2010**, *195* (1−3), 68–72.

(14) Seiler, W.; Wetzel, H.; Hillert, A.; Schollnhammer, G.; Langer, M.; Barlage, U.; Hiemke, C. Pharmacokinetics and bioavailability of benperidol in schizophrenic patients after intravenous and two different kinds of oral application. *Psychopharmacology (Berl)* **1994**, *116* (4), 457–463.

(15) Tachizawa, H.; Sudo, K.; Sasano, H.; Sano, M. Disposition and metabolism of timiperone in the rat, dog, and monkey. *Drug Metab. Dispos.* **1981**, *9* (5), 442–448.

(16) Desta, Z.; Kerbusch, T.; Soukhova, N.; Richard, E.; Ko, J. W.; Flockhart, D. A. Identification and characterization of human cytochrome P450 isoforms interacting with pimozide. *J. Pharmacol. Exp. Ther.* **1998**, *285* (2), 428–437.

(17) Ward, B. A.; Morocho, A.; Kandil, A.; Galinsky, R. E.; Flockhart, D. A.; Desta, Z. Characterization of human cytochrome P450 enzymes catalyzing domperidone N-dealkylation and hydroxylation in vitro. *Br. J. Clin. Pharmacol.* **2004**, *58* (3), 277–287.

(18) Desta, Z.; Soukhova, N.; Morocho, A. M.; Flockhart, D. A. Stereoselective metabolism of cisapride and enantiomer-enantiomer interaction in human cytochrome P450 enzymes: major role of CYP3A. *J. Pharmacol. Exp. Ther.* **2001**, *298* (2), 508–520.

(19) Khan, K. K.; He, Y. Q.; Domanski, T. L.; Halpert, J. R. Midazolam oxidation by cytochrome P450 3A4 and active-site mutants: An evaluation of multiple binding sites and of the metabolic pathway that leads to enzyme inactivation. *Mol. Pharmacol.* **2002**, *61* (3), 495–506.

(20) Moore, C. D.; Shahrokh, K.; Sontum, S. F.; Cheatham, T. E., 3rd; Yost, G. S. Improved cytochrome P450 3A4 molecular models accurately predict the Phe215 requirement for raloxifene dehydrogenation selectivity. *Biochemistry* **2010**, *49* (41), 9011–9019.